IEEE Access
Multidisciplinary ⋮ Rapid Review ⋮ Open Access Journal

Received February 14, 2021, accepted February 18, 2021, date of publication February 22, 2021, date of current version March 2, 2021.

Digital Object Identifier 10.1109/ACCESS.2021.3061248

Terfenol-D Based Magnetic Field Sensor With Temperature Independence Incorporating Dual Fiber Bragg Gratings Structure

BIYAN ZHAN[1,2], TIGANG NING[1,2], LI PEI[1,2], JING LI[1,2], LING LIU[1,2], XUEKAI GAO[1,2], JIAN XU[1,2], JINGJING ZHENG[1,2], JIANSHUAI WANG[1,2], AND BO AI[3], (Senior Member, IEEE)

[1]Key Laboratory of All Optical Network and Advanced Telecommunication Network of EMC, Beijing Jiaotong University, Beijing 100044, China
[2]Institute of Lightwave Technology, Beijing Jiaotong University, Beijing 100044, China
[3]State Key Laboratory of Rail Traffic Control and Safety, Beijing Jiaotong University, Beijing 100044, China

Corresponding author: Tigang Ning (tgning@bjtu.edu.cn)

This work was supported in part by the National Key Research and Development Program of China under Grant 2020YFB1805802, in part by the National Natural Science Foundation of China under Grant 62005012 and Grant 61827817, and in part by the Beijing Natural Science Foundation under Grant 4192022.

ABSTRACT A magnetic field sensor with temperature insensitivity implemented by two fiber Bragg gratings (FBGs) structure is presented and experimentally demonstrated. In the proposed sensing probe, a Terfenol-D piece is bonded with the same type of two FBGs in different direction relative to magnetic field. Two center wavelengths of the notches of FBG filters are mainly determined by the magnetic field, and the two FBGs experience different magnetic-field-induced strain and the same thermal expansion, leading to the linear relationship between the wavelength drift difference and the magnetic field and temperature insensitivity. By monitoring the shift of the wavelength drift difference, the magnetic field measurement for thermal-insensitive interrogation of the magnetic field sensor can be realized. Owing to its compact and temperature independent advantages, the proposed sensor has potential application especially in the unstable direction of magnetic field. Moreover, the sensor can also serve the purpose of temperature measurement by monitoring one of the center wavelengths. The measured sensitivity of the magnetic field intensity of the proposed sensor is 8.77 pm/mT.

INDEX TERMS Dual fiber Bragg gratings, magnetic field sensor, wavelength drift difference, temperature-insensitive.

I. INTRODUCTION

Magnetic field sensors have attracted increasing interests due to its plenty of applications in navigation, vehicle, current detections, and information storage [1]. Various solutions including anisotropic magnetoresistive sensors [2], fluxgate magnetometer [3], superconducting quantum interference device (SQUID) magnetometers [4] and optically pumped magnetometers [5], have been proposed to implement the magnetic measurement. Although the SQUID magnetometer has demonstrated the highest magnetic field sensitivity at the 10^{-17} T level, the detectors must be operated at strict laboratory conditions, such as cryogenic temperature environment, perfect conducting (zero resistance) material, limiting it practical application. In recent years, fiber magneto-optical sensors have received extensive attention because of their significant advantages of high detection sensitivity, low cost, small size, simple manufacturing process and the immunity to electromagnetic interference. Especially, optical magnetic field sensors have been developed based on magnetic fluids [6]–[8], magnetostrictive effect [9]–[12], superconducting magnet [13] and dual-frequency optoelectronic oscillator [14]. Among various magnetic measurement approaches, optical fiber magnetic field sensors attached to magnetically sensitive materials have been recognized as a promising approach. However, thermal expansion exists in FBG and magnetostrictive material which may result in obvious measuring errors. So far, several methods have been proposed to eliminate thermal effect by discriminating the strain changes with the temperature variation. A dual head

The associate editor coordinating the review of this manuscript and approving it for publication was Leo Spiekman.

FBG sensor has been developed by using a tilted FBG demodulator [15]. In [16], a magnetic field sensing scheme using asymmetric giant magnetoimpedance head (AGMI) with negative feedback was reported, where the effect of the temperature variations could be weakened by monitoring the relationship between voltage and magnetic field. Owing to the nonlinearity in wide dynamic range in magnetic field of AGMI, there are some limitations in high-intensity magnetic field measurement. Ivo M. Nascimento *et al*. demonstrated an approach to measure magnetic fields by means of a FBG Fabry–Perot filter, the demodulation was realized by simply detecting the output optical power [17]. Nevertheless, it is challenging to avoid the effect of thermal fluctuations in traditional schemes where a single-mode fiber Bragg grating is used as the sensing head and demodulation is implemented by monitoring the electrical signal, the wavelength or the optical power. In addition, the shift of the laser wavelength in this method may introduce undesired errors.

On the other hand, owing to the wide range of magnetic field and the instability of temperature variation, it is essential to realize high-performance fiber-optic magnetic field sensors. Thus, several approaches using optical magnetic field sensor with temperature independence have been proposed. For instance, by inserting an extra optical fiber without special processing in one arm of the Mach–Zehnder interferometer, the magnetic field sensor decreases the effect of temperature changes [18]. However, the sensor ignores the thermal effect of giant magnetostrictive material. For another method to reduce the effect of temperature on the measurement of magnetic field, [19] proposed two FBGs for simultaneous magnetic field and temperature measurement, and one of them is encapsulated in an alumina tube to compensate the ambient temperature variation. For another temperature-compensated magnetic field sensor [20], two FBGs are bonded on two different alloys respectively for dc magnetic fields and temperature discrimination. Nevertheless, the thermal effect of different materials cannot be exactly the same. Thus, the two methods are unthoughtful in practice. Although a novel magnetostrictive current sensor is proposed to realize temperature compensation [21], [22], the dual-FBGs or multi gratings configuration depends on the orthogonal magnetostriction direction of two giant magnetostrictive materials and the direction of magnetic field, which leads to non-linear negative magnetostriction. Therefore, to further improve the performance of the fiber grating sensors for magnetic field measurement in the confined space and harsh environment, a novel sensing probe with high integration and temperature independence is highly desired.

In this paper, we report a temperature-insensitive magnetic field sensor based on two FBGs theoretically and experimentally, which is independent of the applied magnetic field direction and more integrated of the magnetic field measurement compare to traditional temperature- compensated magnetic field sensor. By analyzing the magnetic-field-induced strain of the Terfenol-D piece in any direction relative to magnetostriction, the best direction of a fiber Bragg grating can be obtained to realize the optimal performance in magnetic field measurement. The two FBGs with nearly the same center wavelength provide the possibility to achieve the temperature-independent measurement. The method offers approximately identical temperature sensitivities and different sensitivities of axial strain for the two different direction of the magnetic field. By incorporating the two FBGs structure with a Terfenol-D piece, the difference between the wavelength drifts of the two FBGs would correspond to the change of magnetic field. Since the two FBGs experience different intensity of magnetic field and the same thermal expansion during the measurement, the magnetic field intensity can be detected by the wavelength drift difference with temperature independence. The ambient temperature can be also measured by the one of wavelength shifts if needed. Hence, the intensity of the magnetic field can be monitored by simply observing the wavelength drift difference.

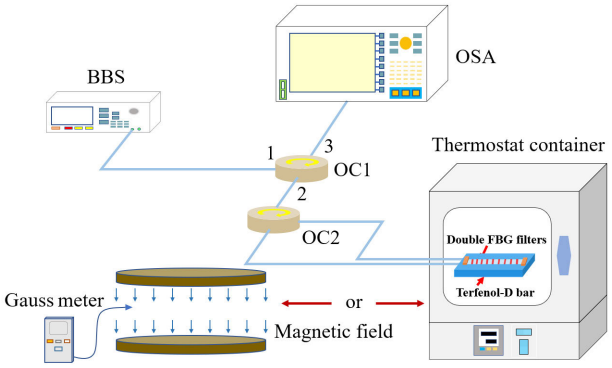

FIGURE 1. Configuration of the magnetic field sensing system with temperature independence. BBS: Broadband source; OC: optical circulator; OSA: optical spectrum analyzer.

II. PRINCIPLE

The schematic diagram of the proposed magnetic field sensor based on the two FBGs structure is illustrated in Fig. 1. The light wave from broadband source (BBS) is sent to the two FBGs through two optical circulator (OC). For the proposed wavelength modulated fiber optic magnetic field sensor, two FBGs bonded on the magnetostrictive material are placed in the magnetic field to be measured. In practice, the two FBGs are slightly stretched before being glued onto the Terfenol-D piece in order to achieve the high stress transmission (subsequently the high mechanical coupling under the stimulus of magnetic fields), and there is no negative magnetostriction along the directions of the two FBGs. Owing to the magnetostriction of the magnetostrictive material, the Terfenol-D piece deforms, introducing the magnetic field-related strain to the two FBGs. And subsequently, the reflected wavelengths of the two FBGs shift with the intensity of magnetic field. Therefore, the optical signals modulated by the magnetic field are reflected and monitored by an optical spectrum analyzer (OSA).

In our design, there are two FBGs bonded on a Terfenol-D piece. In the liner range of the strain induced by the applied

magnetic field ΔB, $\Delta\varepsilon$ can be expressed as $k\Delta B$, where k is a coefficient proportional to the magnetostrictive constant of Terfenol-D [23]. The center wavelength λ_B of FBG sensor is related to strain $\Delta\varepsilon$ and temperature variation ΔT. Therefore, the wavelength shift $\Delta\lambda_B$ depends on the thermal expansion coefficient α_M ($\approx 12\times10^{-6}/^{\circ}C$) of Terfenol-D and ambient temperatures [20], which can be described as:

$$\Delta\lambda_B = (1-P_e)\,\lambda_B k\Delta B + [(\alpha_M-\alpha_F)(1-P_e)+\alpha_F+\xi]\,\lambda_B\Delta T, \quad (1)$$

where α_M and α_F are the thermal expansion coefficient of Terfenol-D and the fiber, respectively, ξ represents the thermo-optic coefficient of the fiber. For a typical silica fiber, the effective elastic-optic coefficient constant P_e is about 0.22.

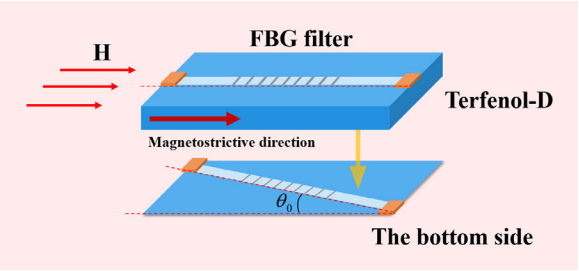

FIGURE 2. Schematic diagram of the sensing probe based on a dual FBGs structure.

The key component in the proposed magnetic field sensor is illustrated in Fig. 2, and the two FBGs have nearly the same center wavelength λ_B. The magnetic field direction is parallel to the magnetostrictive direction of Terfenol-D. One of FBGs (FBG1) is bonded to the Terfenol-D piece along the magnetostrictive direction of Terfenol-D piece to optimize the magnetic field sensitivity, while the other one (FBG2) is bonded with a certain angle θ_0 to the magnetostrictive direction of the Terfenol-D piece. In this case, the strains induced by the thermal expansion effect of Terfenol-D and the thermal expansion effect of optical fiber for both FBGs are identical, while the strain ($k\Delta B, T(\theta_0)\cdot\Delta B$) induced by the magnetic field and the magnetostriction of the magnetostrictive material for the two FBGs are different [24], where $T(\theta_0)$ is a strain coefficient related to the angle θ_0. When changing the angle θ_0 to 90 degrees, the FBG stuck along the angle detected the strain resulted from a negative magnetostriction in this orientation. However, the wavelength shift depends on the magnitude of pre-stress putting on the FBG structure. Therefore, in order to better performance of magnetic field measurement and different magnetic field sensitivity, the rotation angle should be set between 0 and 90 degrees.

Additionally, isotropic magnetic materials can be regarded as essentially uniaxial in the magnetic field. In this case, the relation can be expressed by [24], [25]:

$$M = \frac{3}{2}M_s\left(\cos^2\theta-\frac{1}{3}\right), \quad (2)$$

where M is the magnetostriction constants in the direction of the rotation angle θ relative to the length of the Terfenol-D piece, M_s is the saturation magnetostriction constant along the length of Terfenol-D piece.

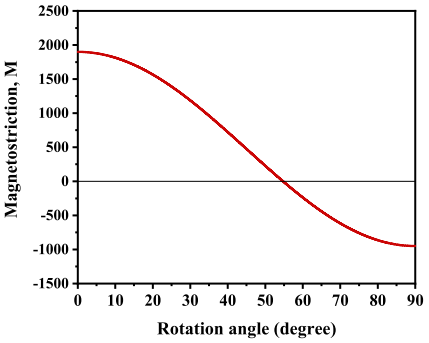

FIGURE 3. Schematic diagram of calculated magnetostriction value of Terfenol-D alloy as a function of a rotation angle.

The calculated magnetostriction of the rotation angle θ range from 0 to 90 degrees for the Terfenol-D is shown in Fig. 3, where the saturation magnetostriction constant of the Terfenol-D is about 1900 ppm.

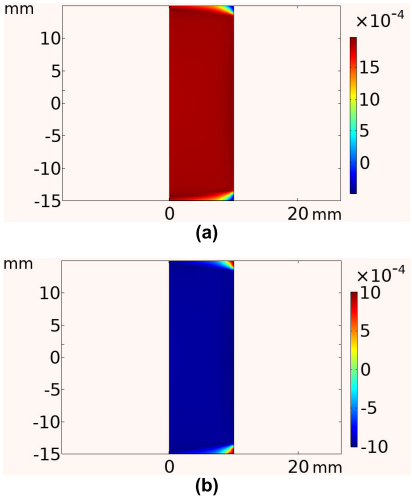

FIGURE 4. Surface plot of the (a) axial and (b) lateral strain component.

Furthermore, the fixture structure is established by using finite element software COMSOL to study the performance of the axial and lateral strain component of the Terfenol-D piece shown in Fig. 4. Due to the symmetric of the geometry structure, the problem is solved as a 2D axisymmetric model, which leads to reduced computation time and the geometric center point of the Terfenol-D piece is used as fixed constrained boundary conditions. Fig. 4 shows that the corresponding strain field caused by the magnetostriction is also fairly uniform in the material. Therefore, the wavelength shift of the magnetic field sensor is conceived of as almost independent of the fixed position of the FBG paralleled to the magnetostrictive direction. Besides, from the Fig. 4, the axial and lateral strain tensor agrees well with the calculated strain

when the rotation angle is 90 and 0 degrees according to Fig. 3, respectively.

From Fig. 3, when the deviation angle exceeds 54.5 degrees, the magnetostriction constant M shifts to a negative magnetostriction, and the values drop as the deviation angle increases. The performance of the wavelength shift depends on the magnitude of pre-stress putting on the FBG structure, which may perform nonlinear behaviors especially under the applied strong magnetic field. Therefore, the suitable range of deviation angle is given less than 54.5 degrees according to the Fig. 3 but greater than 0 degrees to obtain different magnetic field sensitivity, and wavelength in which the grating can work effectively.

Besides, since the wavelength drifts $\Delta\lambda_{B1}$ and $\Delta\lambda_{B2}$ are far less than the initial wavelengths λ_{B1} and λ_{B2}. So, the wavelength difference $\Delta\lambda_B$ can be expressed by:

$$\Delta\lambda_B = \Delta\lambda_{B1} - \Delta\lambda_{B2} = \lambda_B (1 - P_e) [1 - T(\theta_0)] k \Delta B. \quad (3)$$

As can be seen from (3), the two reflected optical signals experience different wavelength drift, and the wavelength drift difference is only determined by the variation of the magnetic field ΔB, which is independent of temperature.

Therefore, the variation of the frequency is linearly proportional to the magnetic field intensity. Thus, the detection of magnetic field variation is performed by simplymonitoring the center wavelength drift difference. Moreover, the ambient temperature changes also can be obtained. Thus, the applied magnetic field and temperature variation can be calculated by

$$\begin{pmatrix} \Delta\lambda_{B1} \\ \Delta\lambda_B \end{pmatrix} = \begin{pmatrix} (1 - P_e)\lambda_B k & \beta_t \lambda_B \\ \lambda_B (1 - P_e)[1 - T(\theta_0)] k & 0 \end{pmatrix} \begin{pmatrix} \Delta B \\ \Delta T \end{pmatrix} = \begin{pmatrix} K_{B1} & K_{T1} \\ K_{B2} & 0 \end{pmatrix} \begin{pmatrix} \Delta B \\ \Delta T \end{pmatrix}, \quad (4)$$

where $K_{B1,2}$ and K_T are the sensitivity of magnetic field and temperature, respectively. Based on the theoretical analysis mentioned above, the magnetic field can be measured accurately by monitoring the wavelength drift difference between the two FBGs with a wide range of temperature, and the temperature variation can also be obtained.

III. EXPERIMENT RESULTS AND DISCUSSION

The experimental setup of our proposed magnetic field sensor is shown in Fig. 1. In our experiment, the highlight of our sensing scheme is the two FBGs structure based on Terfenol-D shown in Fig. 5. It consists of two FBGs with almost identical center wavelength and a Terfenol-D piece (TbDyFe, 5 mm×20 mm×30 mm, Shijiazhuang Saining Electronic Technology Co. LTD). The two FBGs are written in a hydrogen-loaded fiber adopting two identical phase masks with the same pitches through exposure to UV rays. And most importantly, the two FBGs are bonded in different directions on the two opposite sides of the Terfenol-D piece respectively by using UV glue, which result in the different sensitivity of FBGs to magnetic field. Note that the two FBGs are slightly stretched before being glued onto the Terfenol-D piece in order to achieve high mechanical coupling under the stimulus of magnetic field.

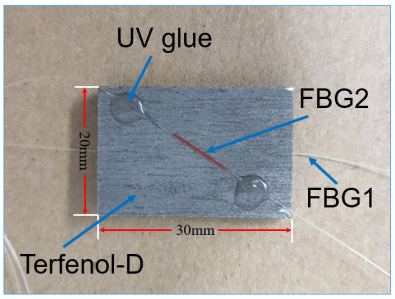

FIGURE 5. The finished magnetic field sensing head.

The reflection spectra of the two FBGs are measured by the OSA. The center wavelengths of the notches of two FBGs are 1540.84 nm and 1541.25 nm as shown in Fig. 6.

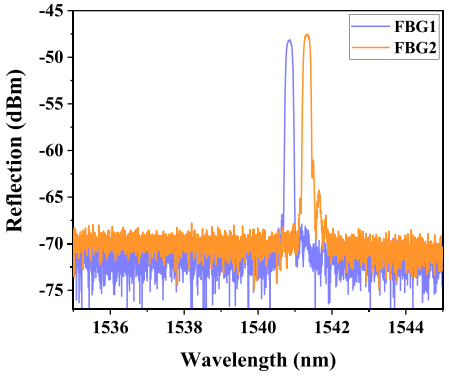

FIGURE 6. Monitored reflectance spectra of the two FBGs.

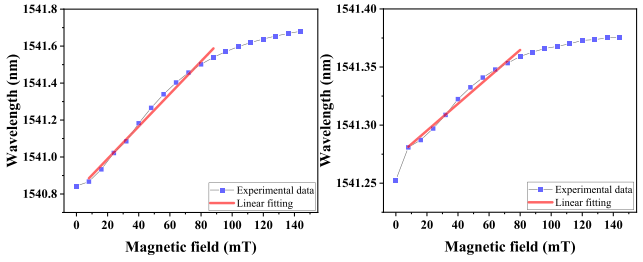

FIGURE 7. The wavelength shift of (a) FBG1 and (b) FBG2 with increasing the applied magnetic field from 0 to 144 mT.

During the properties test, the FBG1 is bonded to the Terfenol-D piece along the magnetostrictive direction of the Terfenol-D, and the FBG2 is bonded with a certain angle 35 degrees relative to the magnetostrictive direction of the Terfenol-D piece shown in Fig. 5. To investigate the sensibility of the two FBGs, the sensing head is tested different magnetic field from 0 to 150 mT with a step of 8 mT. As shown in Fig. 7(a), the range from 8 to 88 mT perform a higher sensitivity and good linear relationship between the wavelength shift of FBG1 and magnetic field. From Fig. 7(b),

the FBG2 wavelength shift and magnetic field has a better linear relationship in the range from 8 to 80 mT compared with the other range. Therefore, the two FBGs display nearly identical magnetic field range for feasible sensibility.

To test the hysteresis of the interrogating system, the sensing probe is placed at the center of two permanent magnets in a certain distance to ensure it will be in uniform magnetic field, and the magnetostriction direction of the Terfenol-D piece works in parallel with the magnetic fields.

In this test, the wavelength shift of the two FBGs with the applied magnetic field increasing and decreasing from 8 to 28 mT are recorded. As shown in Fig. 8(a-d), the wavelength of two FBGs almost returns to the same corresponding position when the applied magnetic field decreases gradually. Fig. 8(e) and (f) show the wavelength shift of the two FBGs linear fitting results in the different magnetic field.

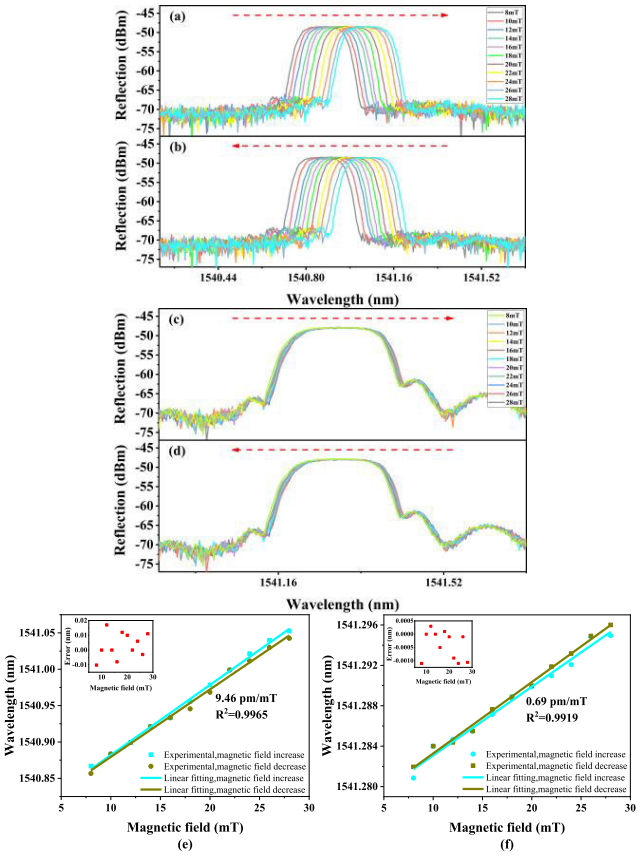

FIGURE 8. The measured reflection spectra of FBG1 which is parallel to magnetic field ((a) the applied magnetic field increases, (b) the applied magnetic field decreases). The measured reflection spectra of FBG2 which is fixed with an angle relative to the magnetic field ((c) the applied magnetic field increases, (d) the applied magnetic field decreases). The relationship between the wavelength shifts of (e) FBG1 and (f) FBG2 and the applied magnetic field (inset: Errors between applied magnetic field increases and decreases measurement).

When the intensity of magnetic field increases at a constant room temperature, the center wavelengths shift to the longer wavelengths at different rates, considering that the two optical signals have different magnetic field sensitivities. Fig. 8(e) and (f) show the relationship between the center

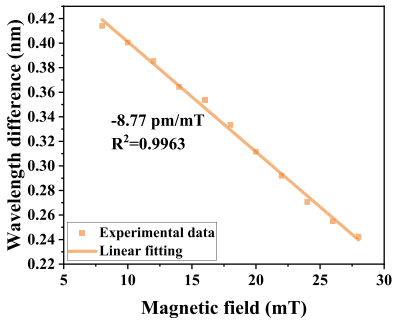

FIGURE 9. The wavelength drift difference versus the magnetic field intensity.

wavelength and the magnetic field intensity. The magnetic field sensitivities measured by the two FBGs are 9.46 pm/mT and 0.69 pm/mT in the range from 8 to 28 mT respectively, and the magnetic field measured by the wavelength drift difference is 8.77 pm/mT shown in Fig. 9.

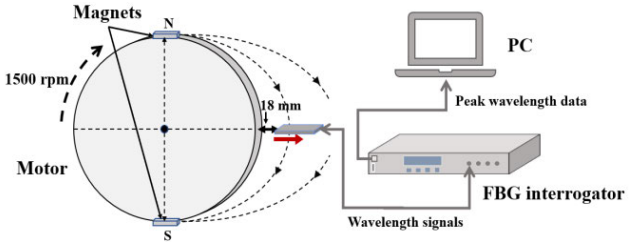

FIGURE 10. Setup used to test the dynamic response of magnetic field sensor.

The test results of the hysteresis of the FBG interrogation show a good agreement respond to the increase and decrease of the magnetic field. The dynamic response performance examination of the magnetic field sensor was performed by analyzing its operation in an AC magnetic field produced by two same NdFeB magnets attached to a wheel driven by three-phase asynchronous motor, spinning at rated speed of 1500 rpm. As shown in Fig. 10, the two magnets were fixed to the wheel, and the sensing probe is fixed axially at a distance of 18 mm from the wheel, where the intensity of magnetic field is measured at 17.2 mT. As shown in Fig. 10, when the two magnets rotate to 90 degrees with the sensing probe, the intensity of magnetic field on the vertical plane relative to two magnets is zero theoretically (actually measured at 0.38 mT). On the other hand, the two FBGs are bonded with the one Terfenol-D, so we can just measure the dynamic response of the one of FBGs owing to their simultaneous interrogation. In this test, the peak wavelength of the FBG along the length of Terfenol-D piece is recorded by a fiber grating sensor interrogator when the wheel spins in steady state shown in Fig. 11.

From Fig. 11, the magnetic field pulse is observed as each magnet pole passes in front of the sensor, and the measured rise time is about 1.4 ms (measured from 10% to 90%), including the rotational latency of the magnets and the sensor

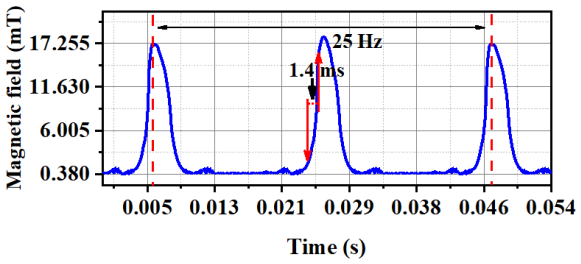

FIGURE 11. The periodical magnetic field pulse measured by the sensor is interrogated by the fiber grating sensor interrogator at a rate of 5 KHz.

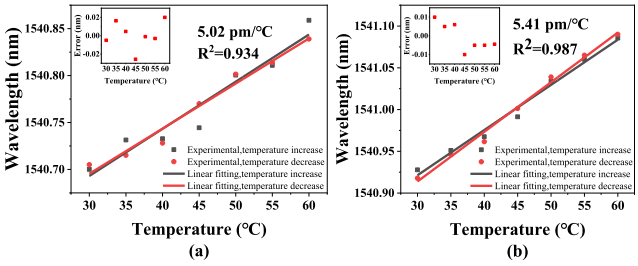

FIGURE 12. The measured wavelength drifts of (a) FBG1 and (b) FBG2 versus the temperature when the magnetic field is not applied (inset: Errors between temperature increases and decreases measurement).

response rise time. Additionally, the rotation angle of the magnetic field intensity from 10% to 90% is measured as 12 degrees, so the rise time of the sensor can be calculated approximately as 67 μs which is far less than the rotational latency of the magnets. Therefore, a case study shows that the magnetic field sensor realizes the magnetic field measurement of dynamic objects respond to the rapidly changing magnetic field pulse.

For temperature sensitivity measurement, the sensing probe is located in the thermostat container to achieve different temperature from 30 °C to 60 °C with a step of 5 °C without the effect of magnetic field. From Fig. 12(a) and (b), when increasing the temperature in the absence of magnetic field, the reflected wavelength of the two FBGs shift to longer wavelength, while the reflected wavelength of the two FBGs shift to the lower wavelength at nearly the same rate when the ambient temperature decreases. The temperature sensitivities measured by the two FBGs are 5.41 pm/°C and 5.02 pm/°C, respectively, showing nearly the same temperature sensitivities. Compared to a typical FBG of its free status, however, the temperature sensitivity of the two constrained FBGs are reduced. Owing to the thermal instability of the UV glue, the change of FBG-GMM mechanical coupling strength under high ambient temperature will cause the pre-stretched FBGs to contract slightly. This is the primary factor of the sensitivity difference. However, the two FBGs experience almost the same contraction according to the temperature test, and this instability can be neglected. The low temperature sensitivity measured by the wavelength drift difference of 0.389 pm/°C is obtained shown in Fig. 13, illustrating

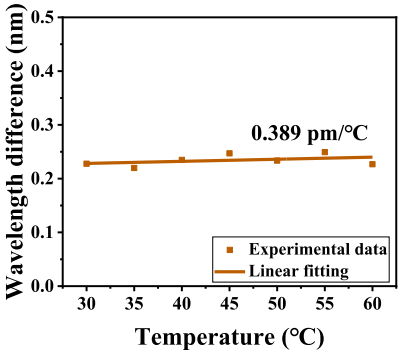

FIGURE 13. The wavelength drift difference versus the temperature when the magnetic field is not applied.

a potential way to implement the temperature-independent magnetic field sensing.

By analyzing the slopes of the wavelengths of the two FBGs and wavelength drift difference, the change of magnetic field can be calculated by (3). The change of temperature also can be obtained simultaneously by (4). Therefore, the relationship of the two FBGs reflection wavelengths, temperature, and magnetic field can be written as

$$\begin{pmatrix} \Delta\lambda_{B1} \\ \Delta\lambda_{B} \end{pmatrix} = \begin{pmatrix} 9.64 & 5.41 \\ 8.96 & 0 \end{pmatrix} \begin{pmatrix} \Delta B \\ \Delta T \end{pmatrix}. \tag{5}$$

In the proposed magnetic field sensor, the two identical FBGs are fully integrated together to ensure the same variation of the environment parameters, i.e. the same ambient temperature variation and the same magnetic field variation. As a result, the wavelength shifts of the two notches of the FBGs are almost the same. To further verify the performance of thermal-insensitive interrogation of wavelength drift difference between the notches during the measurement of magnetic field, it is necessary to analysis the interaction effects on the wavelength drift difference between the magnetic field and temperature.

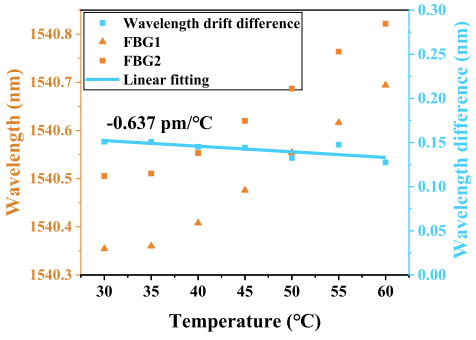

FIGURE 14. The drifts of the center wavelengths of the two FBGs and their wavelength drift difference measured in a magnetic field (the intensity of magnetic field is set at 12 mT) at different temperature.

Next, the temperature sensitivity under a certain magnetic field is measured. The intensity of magnetic field is fixed at 12 mT and the temperatures changes from 30 °C to 60 °C simultaneously. The corresponding experimental results are shown in Fig. 14. Compared with the temperature sensitivity

of 0.389 pm/°C, the temperature sensitivity under the magnetic field obtained by monitoring the wavelength drift difference of 0.637 pm/°C is slightly higher. However, it still far less than the wavelength drift difference shift induced by the magnetic in a certain temperature range.

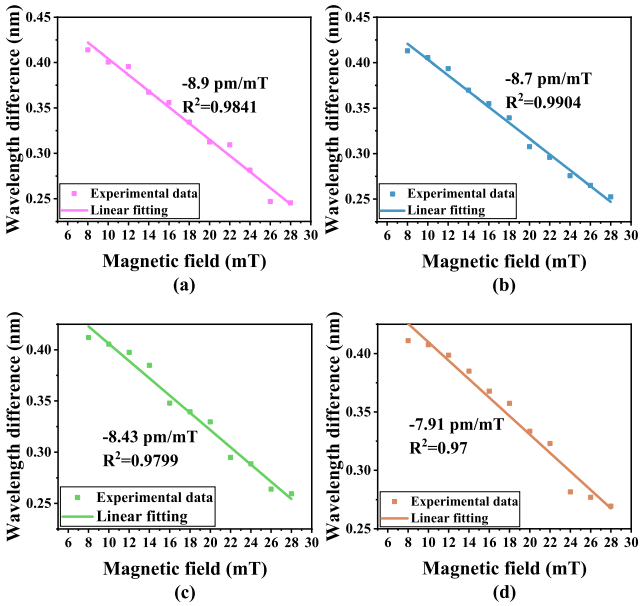

FIGURE 15. The drifts of wavelength difference between the two FBGs' reflection wavelengths measured with the increasing magnetic field at the temperature of (a) 30°C, (b) 40°C, (c) 50°C, and (d) 60°C.

The magnetic field sensitivities of the wavelength drift difference are measured at different temperature next. As shown in Fig. 15, the magnetic field sensitivities of the wavelength drift difference are 8.9 pm/mT, 8.7 pm/mT, 8.43 pm/mT, and 7.91 pm/mT when the temperatures are 30 °C, 40 °C, 50 °C and 60 °C, respectively. The magnetic field sensitivities of the sensing probe are slightly different at different temperatures. The major reason given for the tiny difference is that the two magnetostriction coefficients to field-induced strain nonlinearly change with temperature [26].

In addition, for the FBG which is parallel to the magnetic field, the temperature sensitivity is 5.4 pm/°C, and the relative measurement error of 1 mT introduced by the temperature change in the magnetic field measurement reach as high as 56% with one-degree Celsius change. For the proposed sensing scheme, the relative measurement error is just 0.33% by analyzing the experimental data from 30 °C to 60 °C. By comparing the wavelength shifts under the different temperature conditions, these difference sensitivities are far less than the temperature sensitivities of the wavelength shift of the two FBGs. Therefore, the presented magnetic field sensor dramatically decreases the effect of the ambient temperature variations. This performance can maintain high measurement accuracy even though external temperature fluctuates.

IV. CONCLUSION

In this paper, we have presented and experimentally demonstrated thermal-insensitive magnetic field sensor based on a Terfenol-D piece incorporating the same type of two FBGs with almost the same center wavelength. The special feature of the sensing probe can effectively avoid thermal expansion effect from the Terfenol-D and FBGs. The proposed sensing structure maps the magnetic field and temperature applied to the two FBGs into wavelength shifts. The temperature independent sensing was realized by the two FBGs boned in different direction relative to magnetic field. By monitoring the wavelength drift difference as external temperature fluctuates, the magnetic field intensity can be measured. The temperature measurement also can be obtained if needed. Therefore, the proposed sensor has the advantage of better adaptive capacity to harsh environments. In the practice application, the proposed sensing head can be incorporated into OEO-based system to further increase the detection sensitivity of magnetic field.

REFERENCES

[1] J. Lenz and S. Edelstein, "Magnetic sensors and their applications," *IEEE Sensors J.*, vol. 6, no. 3, pp. 631–649, Jun. 2006.
[2] T. McGuire and R. Potter, "Anisotropic magnetoresistance in ferromagnetic 3D alloys," *IEEE Trans. Magn.*, vol. MAG-11, no. 4, pp. 1018–1038, Jul. 1975.
[3] P. Ripka, "Advances in fluxgate sensors," *Sens. Actuators A, Phys.*, vol. 106, nos. 1–3, pp. 8–14, Sep. 2003.
[4] R. L. Fagaly, "Superconducting quantum interference device instruments and applications," *Rev. Sci. Instrum.*, vol. 77, no. 10, Oct. 2006, Art. no. 101101.
[5] N. Mizutani and T. Kobayashi, "Magnetic field vector detection in frequency domain with an optically pumped atomic magnetometer," *IEEE Trans. Magn.*, vol. 48, no. 11, pp. 4096–4099, Nov. 2012.
[6] X. Li, R. Ma, and Y. Xia, "Magnetic field sensor exploiting light polarization modulation of microfiber with magnetic fluid," *J. Lightw. Technol.*, vol. 36, no. 9, pp. 1620–1625, May 1, 2018.
[7] Y. Chen, Q. Han, W. Yan, Y. Yao, and T. Liu, "Magnetic field and temperature sensing based on a macro-bending fiber structure and an FBG," *IEEE Sensors J.*, vol. 16, no. 21, pp. 7659–7662, Nov. 2016.
[8] L. Bao, X. Dong, S. Zhang, C. Shen, and P. P. Shum, "Magnetic field sensor based on magnetic fluid-infiltrated phase-shifted fiber Bragg grating," *IEEE Sensors J.*, vol. 18, no. 10, pp. 4008–4012, May 2018.
[9] A. Masoudi and T. P. Newson, "Distributed optical fiber dynamic magnetic field sensor based on magnetostriction," *Appl. Opt.*, vol. 53, no. 13, pp. 2833–2838, May 2014.
[10] F. V. B. de Nazare and M. M. Werneck, "Compact optomagnetic Bragg-grating-based current sensor for transmission lines," *IEEE Sensors J.*, vol. 15, no. 1, pp. 100–109, Jan. 2015.
[11] Y. Guo, Y. Zhang, H. Su, F. Zhu, G. Yi, and J. Wang, "Magnetic-field tuning whispering gallery mode based on hollow microbubble resonator with Terfenol-D-fixed," *Appl. Opt.*, vol. 58, no. 32, pp. 8889–8893, Nov. 2019.
[12] J. D. Lopez, A. Dante, A. O. Cremonezi, R. M. Bacurau, C. C. Carvalho, R. C. da Silva Barros Allil, E. C. Ferreira, and M. M. Werneck, "Fiber-optic current sensor based on FBG and Terfenol-D with magnetic flux concentration for enhanced sensitivity and linearity," *IEEE Sensors J.*, vol. 20, no. 7, pp. 3572–3578, Apr. 2020.
[13] H. Zhang, Q. Wang, H. Wang, S. Song, B. Zhao, Y. Dai, G. Huang, and Z. Jiang, "Fiber Bragg grating sensor for strain sensing in low temperature superconducting magnet," *IEEE Trans. Appl. Supercond.*, vol. 20, no. 3, pp. 1798–1801, Jun. 2010.
[14] B. Wu, M. Wang, Y. Dong, Y. Tang, H. Mu, H. Li, B. Yin, F. Yan, and Z. Han, "Magnetic field sensor based on a dual-frequency optoelectronic oscillator using cascaded magnetostrictive alloy-fiber Bragg grating-Fabry Perot and fiber Bragg grating-Fabry Perot filters," *Opt. Exp.*, vol. 26, no. 21, pp. 27628–27638, Oct. 2018.
[15] S. C. Kang, S. Y. Kim, S. B. Lee, S. W. Kwon, S. S. Choi, and B. Lee, "Temperature-independent strain sensor system using a tilted fiber Bragg grating demodulator," *IEEE Photon. Technol. Lett.*, vol. 10, no. 10, pp. 1461–1463, Oct. 1998.

[16] S. Soo Yoon, P. Kollu, D. Young Kim, G. Woo Kim, Y. Cha, and C. Kim, "Magnetic sensor system using asymmetric giant magnetoimpedance head," *IEEE Trans. Magn.*, vol. 45, no. 6, pp. 2727–2729, Jun. 2009.
[17] I. M. Nascimento, J. M. Baptista, P. A. S. Jorge, J. L. Cruz, and M. V. Andres, "Intensity-modulated optical fiber sensor for AC magnetic field detection," *IEEE Photon. Technol. Lett.*, vol. 27, no. 23, pp. 2461–2464, Dec. 1, 2015.
[18] N. Zhang, M. Wang, B. Wu, M. Han, B. Yin, J. Cao, and C. Wang, "Temperature-insensitive magnetic field sensor based on an optoelectronic oscillator merging a Mach–Zehnder interferometer," *IEEE Sensors J.*, vol. 20, no. 13, pp. 7053–7059, Jul. 2020.
[19] K. D. M. Sousa, R. Zandonay, E. V. D. Silva, C. Martelli, and J. Silva, "Application of fiber Bragg grating to determine the Terfenol-D magnetostriction characteristics for sensor development," *J. Microw., Optoelectron. Electromagn. Appl.*, vol. 13, no. 1, pp. 1–9, 2015.
[20] J. Mora, A. Diez, J. L. Cruz, and M. V. Andres, "A magnetostrictive sensor interrogated by fiber gratings for DC-current and temperature discrimination," *IEEE Photon. Technol. Lett.*, vol. 12, no. 12, pp. 1680–1682, Dec. 2000.
[21] H. García-Miquel, D. Barrera, R. Amat, G. V. Kurlyandskaya, and S. Sales, "Magnetic actuator based on giant magnetostrictive material Terfenol-D with strain and temperature monitoring using FBG optical sensor," *Measurement*, vol. 80, pp. 201–206, Feb. 2016.
[22] J. Han, H. Hu, H. Wang, B. Zhang, X. Song, Z. Ding, X. Zhang, and T. Liu, "Temperature-compensated magnetostrictive current sensor based on the configuration of dual fiber Bragg gratings," *J. Lightw. Technol.*, vol. 35, no. 22, pp. 4910–4915, Nov. 15, 2017.
[23] Y. Yang, Q. Yang, W. Ge, and L. Li, "A temperature-insensitive AC current sensor based on two opposite bias magnetic circuits," *IEEE Photon. Technol. Lett.*, vol. 28, no. 23, pp. 2724–2727, Dec. 1, 2016.
[24] S.-M. Na, J. Eng-Morris, J. Downing, and A. B. Flatau, "Crystal orientation dependence of magnetization and magnetostriction behaviors in highly textured galfenol and alfenol thin sheets," *IEEE Trans. Magn.*, vol. 53, no. 11, Nov. 2017, Art. no. 2503104.
[25] P. T. Squire, "Magnetomechanical measurements of magnetically soft amorphous materials," *Meas. Sci. Technol.*, vol. 5, no. 2, pp. 67–81, Feb. 1994.
[26] N. Ranvah, I. C. Nlebedim, Y. Melikhov, J. E. Snyder, D. C. Jiles, A. J. Moses, and P. I. Williams, "Temperature dependence of magnetostriction of $Co_{1+x}Ge_xFe_{2-2x}O_4$ for magnetostrictive sensor and actuator applications," *IEEE Trans. Magn.*, vol. 44, no. 11, pp. 3013–3016, Nov. 2008.

BIYAN ZHAN was born in Hubei, China. He received the B.S. degree in information and computing science from Henan Polytechnic University, China, in 2017. He is currently pursuing the master's degree with Beijing Jiaotong University. His research interests include microwave photonic generator, optomagnetic sensor, and radio-over-fiber communication systems.

TIGANG NING received the Ph.D. degree in telecommunication and information system from Northern Jiaotong University, Beijing, China, in 2003. He is currently a Professor with the School of Electronics and Information Engineering, Beijing Jiaotong University. His recent research interests include all-optical networking, high-power fiber laser, and radio-over-fiber communication systems.

LI PEI was born in Shanxi, China. She is currently a Professor with the School of Electronics and Information Engineering, Beijing Jiaotong University, Beijing, China. Her current research interests include high-speed optical telecommunication networks, optical fiber sensor, radio-over-fiber communication systems, and novel optical devices.

JING LI received the B.E. degree in communication engineering from the People's Liberation Army, Academy of Communication and Commanding, Wuhan, China, in 2006, the M.E. degree in electromagnetic field and microwave technology from the Communication University of China, Beijing, China, in2008, and the Ph.D. degree in communication and information system from Beijing Jiaotong University, Beijing, in 2013. His research interests include microwave photonic generator and radio-over-fiber communication systems.

LING LIU received the B.S. degree in communications engineering from the Changsha University of Science and Technology, Changsha, China, in 2016. She is currently pursuing the Ph.D. degree with the Key Laboratory of All Optical Network and Advanced Telecommunication Network, Ministry of Education, Institute of Lightwave Technology, Beijing Jiaotong University, Beijing, China. She is also a Joint Training Student in electrical and computer engineering with McGill University, Montreal, QC, Canada. Her current research interests include microwave photonic filters, optoelectronic oscillators, and their application in sensing.

XUEKAI GAO received the B.S. degree in electronic information science and technology from Qufu Normal University, Qufu, China, in 2013. He is currently pursuing the Ph.D. degree in communication and information system with Beijing Jiaotong University. His research interests include modal interference-based guided wave devices and integrated optical devices.

JIAN XU was born in Hebei, China. He is currently pursuing the Ph.D. degree in communication and information system with Beijing Jiaotong University. His research interests include optical fiber sensor and integrated optical devices.

JINGJING ZHENG was born in Henan, China. She is currently an Associate Professor with the School of Electronics and Information Engineering, Beijing Jiaotong University, Beijing, China. Her current research interests include specialty fiber and components, optical fiber sensor, and novel optical devices.

JIANSHUAI WANG was born in Hebei, China, in 1989. He is currently an Associate Professor with the School of Electronics and Information Engineering, Beijing Jiaotong University, Beijing, China. His current research interests include devices based on special optical fibers, optical fiber sensor, and high-power fiber laser.

BO AI (Senior Member, IEEE) received the Ph.D. degree in telecommunication and information system from Xidian University, Beijing, China, in 2004. He is currently a Professor with the Key Laboratory of All Optical Network and Advanced Telecommunication Network of Ministry of Education, Beijing Jiaotong University, Beijing. His recent research interests include broadband mobile communication systems and dedicated mobile communications.